

Development and Radiolabeling Evaluation of ¹⁷⁷Lutetium-Tedizolid

Merve KARPUZ[°], Emre OZGENC^{**}, Evren GUNDOGDU^{***}, Zeynep BURAK^{****}

Development and Radiolabeling Evaluation of ¹⁷⁷Lutetium-Tedizolid

SUMMARY

Infection diseases is still one of the major health problems all around the world. Early diagnosis and differentiation of infection from other pathological conditions such as cancer and inflammation play a critical role in treating the infection in acute stages. Imaging techniques using in the infection diagnosis present some advantages such as, the ability to image the whole body, the detection of focal location and stage, and following up on infection. Although various antibiotics can be used in the treatment, there are some problems including serious side effects of antibiotics or the development of antimicrobial resistance in the clinics. In our study, tedizolid, a second-generation oxazolidinone antibiotic, was radiolabeled with ¹⁷⁷Lu radionuclide to develop a theranostic agent against gram-positive bacterial infections. The radiolabeling was performed under room conditions, and labeling efficiency and stability were evaluated by paper chromatography and HPLC. The optimum incubation period was found as 60 min to obtain high radiolabeling efficiency. Different mobile and stationary phases in paper chromatography were tested to determine the radiochemical impurities in ¹⁷⁷Lu-TDZ solution, and ITLC-SG was found to be proper as the stationary phase. In addition, ammonium hydroxide: methanol: water, and DTPA solutions were chosen as mobile phases. In the HPLC chromatogram, two different peaks were observed depending on the retention times of the free ¹⁷⁷Lu and ¹⁷⁷Lu-TDZ complex. Unfortunately, over 80% purity values were not obtained in the results of radiolabeling stability analyses; therefore, the addition of a chelating agent in the radiolabeling condition was suggested to increase the stability.

Key Words: lutetium-¹⁷⁷, tedizolid, theranostic, infectious diseases

¹⁷⁷Lutetium-Tedizolid'in Geliştirilmesi ve Radyoışaretlenmesi

ÖZ

Enfeksiyon hastalıkları hala dünyada temel sağlık problemlerinden birini oluşturmaktadır. Enfeksiyonun erken aşamalarda teşhisi ve kanser veya inflamasyon gibi diğer patolojilerden ayrımı, enfeksiyonu akut aşamalarda tedavi etmede kritik rol oynamaktadır. Enfeksiyon teşhisinde kullanılan görüntüleme yöntemleri tüm vücut görüntüsü alabilme, enfeksiyonu odağını ve evresini tespit edebilme ve hastalığı izleyebilme gibi avantajlara sahiptir. Enfeksiyon tedavisinde çeşitli antibiyotikler kullanılmasına rağmen, klinikte antibiyotiklerin ciddi yan etkileri ve antimikrobiyal direnç gelişimi gibi problemler mevcuttur. Çalışmamızda enfeksiyon için teranostik bir ajan geliştirme amacıyla gram pozitif bakterilere karşı etkili ikinci nesil oksazolidinon antibiyotiği olan tedizolid, ¹⁷⁷Lu radyonüklidi ile radyoışaretlenmiştir. Radyoışaretleme, oda koşullarında gerçekleştirilmiş ve işaretleme etkinliği ile stabilitesi, kağıt kromatografisi ve HPLC ile değerlendirilmiştir. Yüksek radyoışaretleme verimi elde etmek için optimum inkübasyon süresi 60 dakika olarak bulunmuştur. ¹⁷⁷Lu-TDZ çözeltisindeki radyokimyasal safsızlıkları belirleme amacıyla kağıt kromatografisi için farklı mobil ve sabit fazlar test edilmiş ve sabit faz olarak ITLC-SG uygun bulunmuştur. Ayrıca amonyum hidroksit: metanol: su ve DTPA çözeltileri mobil faz olarak seçilmiştir. HPLC kromatogramında serbest ¹⁷⁷Lu ve ¹⁷⁷Lu-TDZ kompleksinin alıkonma sürelerine bağlı olarak iki farklı pik gözlenmiştir. Ne yazık ki, radyoışaretleme stabilitesi testlerinin sonuçlarında %80'in üzerinde saflık değerleri elde edilememiştir, bu nedenle radyoışaretleme ortamına şelat yapıcı ajan eklenmesi önerilmiştir.

Anahtar Kelimeler: lutesyum-¹⁷⁷, tedizolit, teranostik, enfeksiyon hastalıkları

Received: 6.04.2022

Revised: 22.06.2022

Accepted: 16.08.2022

[°] ORCID ID: 0000-0001-6681-2448, Izmir Katip Celebi University Faculty of Pharmacy, Department of Radiopharmacy, Izmir, Turkey.

^{**} ORCID ID: 0000-0002-7586-8520, Ege University Faculty of Pharmacy, Department of Radiopharmacy, Izmir, Turkey.

^{***} ORCID ID: 0000-0003-2111-101X, Ege University Faculty of Pharmacy, Department of Radiopharmacy, Izmir, Turkey.

^{****} ORCID ID: 0000-0002-3187-9447, Ege University Faculty of Medicine, Department of Nuclear Medicine, Izmir, Turkey.

[°] Corresponding Author; Merve KARPUZ,

Tel: +90 232 329 3535, Fax: +90 232 386 08 88, e-mail: merve.karpuz@ikcu.edu.tr, merve-karpuz@hotmail.com

INTRODUCTION

Infection is still one of the major health problems worldwide in view of the global coronavirus disease 2019 (Covid-19). Despite acute respiratory syndrome coronavirus 2 (SARS-CoV-2) causes Covid-19, according to the literature, secondary or concurrent bacterial infections, including *Staphylococcus aureus* (*S. aureus*) co-infections, have been detected in many patients with SARS-CoV-2 (Singh, Upadhyay, Reddy, & Granger, 2021). In addition to SARS-CoV-2, many viral respiratory pathogens (e.g., orthomyxoviruses) are the leading cause of secondary severe bacterial infections such as staphylococcal pneumonia (Mulcahy & McLoughlin, 2016). Hospital-acquired bacterial pneumonia (HABP) and ventilator-associated bacterial pneumonia (VABP) are remarkable burdens on the healthcare system due to mortality rate and the development of antibiotic resistance (Bart, Rubin, Kim, Farley, & Nambiar, 2020). *S. aureus* is one of the commonly identified pathogens in patients with HABP and VABP, and it also can cause various infections such as gastroenteritis, meningitis, osteomyelitis, septic arthritis, or urinary tract infections (Jones, 2010; Tong, Davis, Eichenberger, Holland, & Fowler, 2015). Different antibiotics (e.g., vancomycin, trimethoprim-sulfamethoxazole, linezolid, or teicoplanin) can be chosen depending on methicillin-resistant (MR) or infection syndromes in the management of *S. aureus* infections (Tong et al., 2015). Although vancomycin and linezolid are the first-line therapeutic agents in the treatment of pneumonia caused by MR *S. aureus*, they cause serious side effects such as nephrotoxicity and myelosuppression, respectively (Liu et al., 2011). Moreover, the development of antimicrobial resistance is increasing day by day. In addition to therapy of infection, diagnosis possesses a crucial role in the selection of an appropriate therapeutic agent and treating the infection in acute stages. The infection diagnosis comprises the investigation of patients' samples, the evaluation of patients' symptoms, laboratory tests, and imaging techniques. Imaging

techniques present advantages, such as the ability to image the whole body, the detection of focal location and stage, and the following up of infection. However, they may be inadequate in the differentiation of infection from other pathological cases such as cancer or inflammation. Therefore, the development of effective treatment and imaging options for *S. aureus* is critical for avoiding the progression of infection and decreasing infection-related deaths.

Among imaging techniques, nuclear medicine techniques (gamma camera, positron emission tomography (PET), and single-photon emission tomography (SPECT)) are advantageous systems due to their ability to image the whole body, provide three-dimensional functional and physiological images, and use with other imaging techniques such as magnetic resonance imaging (MRI) or computed tomography (CT) as hybrid systems (PET/CT, PET/MRI, SPECT/CT) (Wu & Shu, 2018). Radiopharmaceuticals, used for diagnosis or therapy of various diseases, contain pharmaceutical parts and radioactive isotopes. They can be used in the diagnosis and therapy of various diseases including infection depending on the radioactive decay type of radionuclides. Infection can be imaged using different radiopharmaceuticals such as ^{67}Ga -citrate, $^{99\text{m}}\text{Tc}$ -diphosphonates, $^{99\text{m}}\text{Tc}/^{111}\text{In}$ l-white blood cells, ^{111}In -biotin in nuclear medicine clinics (Karpuz & Silindir-Gunay, 2022). Radionuclides (e.g., $^{99\text{m}}\text{Tc}$, ^{18}F , ^{68}Ga , ^{123}I , ^{67}Ga , ^{201}Tl), which emit gamma (γ) or positron (β^+) rays, use for imaging purposes, while alpha- (α) or beta- (negatron, β^-) emitting ones (e.g., ^{213}Bi , ^{225}Ac , ^{223}Ra , ^{90}Y) are therapeutic radionuclides (Kassis, 2008; Velikyan, 2014). In addition, some radionuclides, that emit both γ or β^+ and α or β^- , are referred to as theranostic, and they are used for imaging and therapy purposes. Although $^{99\text{m}}\text{Tc}$ radiopharmaceuticals are widely used in nuclear medicine clinics, the development of new radiopharmaceuticals with different radionuclides is required because of the shortage of $^{99\text{m}}\text{Tc}$. The theranostic approach, the combination of therapy and imaging, presents some ad-

vantages, including monitoring the pharmacokinetic/biodistribution profile and the targeting ability of a therapeutic agent, and rapid diagnosis and therapy. Radiopharmaceuticals, containing ^{131}I , ^{177}Lu , ^{111}In , or ^{64}Cu as a radionuclide part, can be used as theranostic molecules (Gutfilen, Souza, & Valentini, 2018; Levine & Krenning, 2017). ^{177}Lu is one of the most widely used theranostic radionuclides due to its gamma photons and beta particulates. The studies regarding ^{177}Lu labeled radiopharmaceuticals have increased in recent years thanks to its advantages such as long physical half-life and large-scale production. $^{177}\text{Lu}^{+3}$ can conjugate with various molecules (e.g., antibodies, peptides, glycoproteins, hydroxyapatite minerals) due to its empty s, p, and d orbitals (Banerjee, Pillai, & Knapp, 2015). Moreover, some ^{177}Lu -radiopharmaceuticals containing antibiotic molecules like kanamycin, bleomycin, benzylpenicillin, sulfadiazine, and colistin were developed in the literature (Akbar et al., 2017; Karpuz et al., 2022; Naqvi et al., 2017; Shahzad et al., 2017; Yousefnia et al., 2010b)

Tedizolid phosphate (TDZ), a second-generation oxazolidinone, was developed for linezolid-resistant *S. aureus* infections. The minimum inhibitory concentration of TDZ has found 8-fold lower compared to linezolid. TDZ, a prodrug, binds bacterial 23S ribosome initiation complex and 50S ribosome subunit to prevent the formation of 70S ribosome complex after its activation by phosphatase in plasma (Cada, Ingram, & Baker, 2014). Although it was approved by the US Food and Drug Administration (FDA) for the treatment of acute bacterial skin and skin structure infection in 2014, its *in vitro* antibacterial effect was also evaluated for tuberculosis, pneumonia, or gas gangrene in the literature (Bryant, Bayer, Aldape, McIndoo, & Stevens, 2020; Srivastava, Cirrincione, Deshpande, & Gumbo, 2020; Wunderink et al., 2021). Although no study has been performed in the literature about radiolabeling of TDZ, linezolid was radiolabeled with ^{18}F to image *Mycobacterium tuberculosis*-infected lungs (Mota et al., 2020).

In light of the information above, in our study, a

pre-radiolabeling process of TDZ with ^{177}Lu was researched to obtain a theranostic radiopharmaceutical against gram-positive bacterial infections. The study's novelty is to radiolabel TDZ with ^{177}Lu , and evaluate the radiolabeling efficiency and stability of the ^{177}Lu -TDZ complex.

MATERIALS AND METHODS

Materials

TDZ was obtained from Wuhan Vanzpharm Inc. (Wuhan, China). $^{177}\text{LuCl}_3$ was obtained from Eczacıbaşı-Monrol Nuclear Products. Diethylenetriamine-pentaacetic acid (DTPA), ethylenediamine-tetraacetic acid (EDTA), ammonium hydroxide, and ammonium acetate were purchased from Sigma-Aldrich. Acetonitrile, and instant thin layer chromatography-silica gel (ITLC-SG) and whatman chromatography papers were obtained from Merck and Agilent, respectively.

Methods

Characterization of TDZ

The characterization studies were performed by ultraviolet spectrum (UV) and Fourier transform infrared (FTIR) analyses to determine TDZ and control its quality. UV spectrum of TDZ in distilled water was obtained between 100 and 400 nm to determine the wavelength of maximum absorption (λ_{max}) using a spectrophotometer (BMG Labtech-Clariostar plus). FTIR analysis was performed using a potassium bromide tablet in the 4000 to 650 cm^{-1} range by a spectrometer (Perkin Elmer Spectrum 100 FT-IR).

Radiolabeling study

To radiolabel TDZ with ^{177}Lu , 1 mL of $^{177}\text{LuCl}_3$ solution with 1 mCi radioactivity was added to the TDZ % 0.9 saline solution with 2.5 $\text{mg}\cdot\text{mL}^{-1}$ concentration. Different incubation periods (5, 30, and 60 min) and filtration effects were evaluated to determine the optimal radiolabeling condition TDZ with ^{177}Lu . For this purpose, radiolabeled mixtures were incubated for 5, 30, and 60 min at room temperature. In addition, after the separation of radiolabeled TDZ

solution into two samples, one of the samples was filtered through a cellulose nitrate membrane filter having a 0.22- μm pore size using a syringe.

Radiolabeling efficiency of ^{177}Lu -TDZ

After the radiolabeling studies, the percentages of radiochemical purity (RCP %) were tested by using paper chromatography for the evaluation of the filtration effect on radiolabeling efficiency, and the determination of the optimum incubation period.

To obtain the RCP % values, ^{177}Lu -TDZ complex

was applied to stationary phases, and the radioactivity values at the origin and front were measured by a dose calibrator (Biodex Atomlab) at the end of the development of mobile phases. Different stationary (ITLC-SG and Whatman 3MM) and mobile phases (Ammonium hydroxide: methanol: water solution (1:20:20, v:v), Ammonium acetate: methanol solution (1:1, v:v), DTPA solution (10 mM), and EDTA solution (50 mM)) which are given in Table 1, were used. The RCP % values of ^{177}Lu -TDZ were calculated by using the following equation:

$$RCP(\%) = \frac{Lu - 177 - TDZ \text{ radioactivity}}{Lu - 177 - TDZ \text{ radioactivity} + Free Lu - 177 \text{ radioactivity}} \times 100$$

Radiolabeling stability of ^{177}Lu -TDZ

The radiolabeling stability of the ^{177}Lu -TDZ complex was evaluated by paper and radio-high pressure liquid chromatography (Radio-HPLC). To that end, RCP % values of the filtered ^{177}Lu -TDZ complex in saline solution were calculated at 0, 1, and 7 days after the radiolabeling procedure.

In the radio-HPLC study, 10 μL volume of ^{177}Lu -TDZ complexes were injected in an HPLC system fitted with a NaI Gamma detector, C18 (Inertsil ODS-3 GL Science 150 \times 3 mm) column, the photodiode array (PDA), and LC Solution software data analyzer (Shimadzu SCL-10A). Elution was obtained using the following gradient steps of solvents A (ultrapure water) and B (acetonitrile) 90:10 for 5 min, then 80:20 for 5 min, then 95:5 for 5 min, and then 90:10 for 5 min at a flow rate of 50 $\mu\text{L}\cdot\text{min}^{-1}$. Analyses were performed at room temperature.

Statistical Analysis

All experiments were performed in triplicates. Data are expressed as the mean \pm the standard deviation of the mean (SD). Differences were examined with Student's t-test using GraphPad Prism 6 program, and statistical significance was set at $p < 0.05$ for all data.

RESULTS AND DISCUSSION

Characterization Results of TDZ

The quality control of drug substances and excipients should be performed to check if the package ingredients obtained from the company are suitable before the preparation of pharmaceutical formulations including radiopharmaceuticals. Therefore, TDZ, used as the pharmaceutical part of the radiolabeled complex, was successfully identified by the UV and FTIR analyses. In the UV analysis, the maximum absorption peak of TDZ was obtained at 290 nm wavelength, as seen in Figure 1. This finding is in agreement with the study in the literature (Yang, Tian, Liu, & Huang, 2018).

The vibrations of different functional groups and bonds obtained by FTIR are founded as compatible with the molecular structure of TDZ, as seen in Figure 2A and Figure 2B. The vibration of C=C stretching and C-C stretching in the phenyl ring of TDZ was detected at 1621 cm^{-1} , similar to the literature (Paczkowska-Walendowska et al., 2020). C=O, C-O, C-C-N, C-C-C, and C-N-C bonds in the oxazolidinone group were shown in 1742, 1090, and 1020 cm^{-1} . The characteristic vibrations of (pyridine-3-yl)phenyl-3-fluoro containing C-C-N bending, C-F, and C-O bands were detected at 1405, 1276, and 1200 cm^{-1} , which is in

agreement with a study (Michalska, Mizera, Lewandowska, & Cielecka-Piontek, 2016). Furthermore, the vibration of the phosphate group ($H_2PO_4^-$) in TDZ is determined in 1214, 1156, 1078, 942, and 883 cm^{-1} of

spectra. These characteristic peaks of the phosphate group were found in similar ranges of spectra to the previous study in the literature (Klähn et al., 2004).

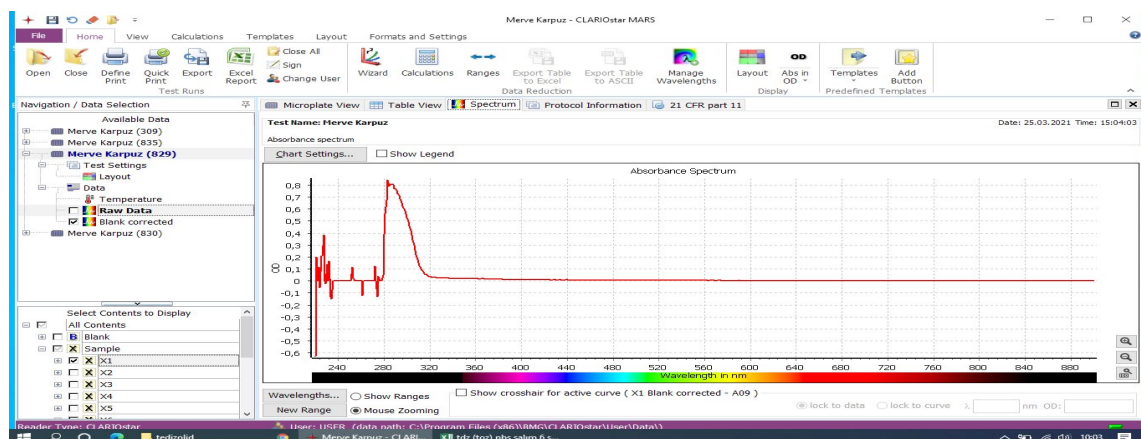


Figure 1. Absorbance spectrum of TDZ.

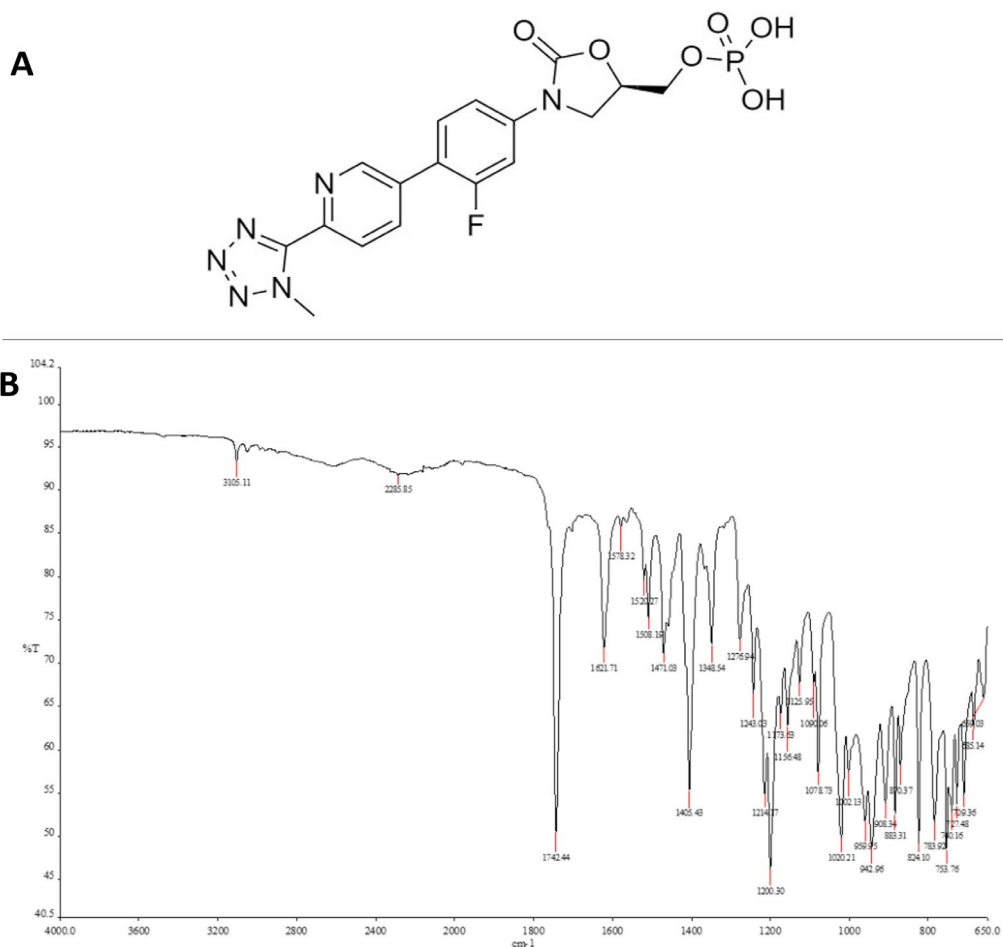


Figure 2. (A) Molecular structure of TDZ (Drawn by using ChemDraw), (B) FTIR spectra of TDZ.

Radiolabeling Study

TDZ was successfully radiolabeled with ^{177}Lu , and the radiochemical purity of the ^{177}Lu -TDZ complex was calculated. After the radiolabeling procedure, radiolabeled complexes should be tested to detect radiochemical impurities such as free radionuclides. Therefore, the amount of free $^{177}\text{Lu}^{+3}$ as the main radiochemical impurity should be calculated for ^{177}Lu radiopharmaceuticals (Banerjee et al., 2015). To separate free $^{177}\text{Lu}^{+3}$, different mobile phases were used. The location of the radiolabeled complex in the chromatography system was found variable depending on using various stationary and mobile phases. The presence of complex ^{177}Lu with DTPA and EDTA caused the elution of free ^{177}Lu to the front, while free ^{177}Lu remained at the origin in the elution system using ammonium hydroxide: methanol: water or ammonium acetate: methanol mobile phases. The R_f value of the free ^{177}Lu was found as 0.8 and 1.0 in DTPA and EDTA mobile phases, respectively. In addition, the R_f value of ^{177}Lu -TDZ complex was calculated as 0.8 for both ammonium hydroxide: methanol: water and ammonium acetate: methanol mobile phases. These results agree with the study in which the R_f value of free $^{177}\text{Lu}^{+3}$ was reported as 0.9 and 0.1 in DTPA solution and ammonium acetate: methanol solution, respectively (Yousefnia et al., 2010a). In the other two studies using ammonium acetate: methanol as a mobile phase, it was reported that free $^{177}\text{Lu}^{+3}$ remained at the origin (Akbar et al., 2017; Xu et al., 2019). Also, EDTA solution was used for the detection of radio-

chemical impurities such as free $^{177}\text{Lu}^{+3}$ at the front of the plate (Naqvi et al., 2017).

Radioactivity values for different incubation times measured at the end of the development of mobile phases in the chromatography system are given in Table 1. The radioactivity values of the ^{177}Lu -TDZ complex were found to be statistically higher in the ammonium hydroxide: methanol: water and ammonium acetate: methanol solutions than that of DTPA and EDTA solutions due to the ^{177}Lu -DTPA/EDTA complex formation ($p < 0.05$). Therefore, the radiochemical impurities were separated using two different solvent systems to calculate the RCP % values of ^{177}Lu -TDZ, and RCP % values were found between 48-87 %, as seen in Table 2. In the literature, similar to our findings, it was reported that the possible ^{177}Lu -DTPA/EDTA complex formation caused the low RCP % values (Yousefnia et al., 2010a). Different incubation periods were tested to obtain high RCP %, and the highest RCP % values (approximately 90%) were obtained in 60 min incubation period, which is in agreement with the incubation time of a ^{177}Lu labeling study in the literature (Hu et al., 2002). In addition, for 30 min incubation period, higher RCP % values were obtained in the chromatography system using ammonium hydroxide: methanol: water and DTPA solutions in a mobile phase ($p < 0.05$). Thus, 60 min and ammonium hydroxide: methanol: water and DTPA solutions were chosen as an optimal incubation time and a mobile phase for the radiolabeling and evaluation of radiolabeling efficiency studies.

Table 1. The radioactivity values at the origin and front of the plate for the ^{177}Lu -TDZ complex in different phases and incubation times.

Mobile phases/ incubation time (min)	Ammonium hydroxide: methanol: water solution			Ammonium acetate: methanol solution			DTPA solution			EDTA solution		
	5	30	60	5	30	60	5	30	60	5	30	60
Origin	0.25 ± 0.08	0.71 ± 0.39	0.145 ± 0.08	0.04 ± 0.03	0.98 ± 0.08	0.05 ± 0.03	0.23 ± 0.16	1.59 ± 0.59	1.69 ± 0.61	0.08 ± 0.07	5.17 ± 0.86	2.8 ± 0.42
Front	3.26 ± 0.06	2.79 ± 0.47	0.65 ± 0.06	1.39 ± 0.06	3.75 ± 0.42	0.87 ± 0.03	2.06 ± 0.37	4.88 ± 3.58	1.145 ± 0.30	1.75 ± 0.37	7.09 ± 0.44	1.22 ± 0.28

Table 2. The RCP% values of ¹⁷⁷Lu-TDZ.

Mobile phases/ incubation times (min)	Ammonium hydroxide: methanol: water solution and DTPA solution			Ammonium acetate: methanol solution and EDTA solution		
	5	30	60	5	30	60
RCP % of ¹⁷⁷ Lu-TDZ complex	76.8 ± 4.5	66.8 ± 3.9	87.1 ± 2.3	80.3 ± 1.5	48.9 ± 2.2	86.1 ± 4.2

The main administration route for radiopharmaceuticals is intravenous injection because of the physical half-life of radionuclides. Therefore, they should be sterilized by filtration using a membrane filter with a 0.22 µm pore size before the injection (Aerts et al., 2014). After the radiolabeling study, the radiolabeled complex was filtrated, and the pH value was evaluated. The pH values of both filtrated and un-filtrated ¹⁷⁷Lu-TDZ complexes were found to be 4.5, which is the optimal pH for the radiolabeling with ¹⁷⁷Lu, according to the literature (Breeman, De Jong, Visser, Erion, & Krenning, 2003; Shahzad et al., 2017; Xu et al., 2019). The filtration effect on RCP % values and radiolabeling stability was evaluated, and the results

are given in Figure 3. No statistically significant difference was observed between RCP % values of filtrated and un-filtrated ¹⁷⁷Lu-TDZ solutions on the 0th and 1st day ($p \geq 0.05$). However, the RCP % value of filtrated solution significantly decreased on the 4th and 7th days after radiolabeling ($p < 0.05$). In our study, the radiolabeled complex was filtrated after the preparation. However, its radiochemical purity was found to be significantly lower compared to the un-filtrated complex. Therefore, it can be suggested that ¹⁷⁷Lu-TDZ solutions should be filtrated just before the administration to avoid this undesirable decrease in radiolabeling stability.

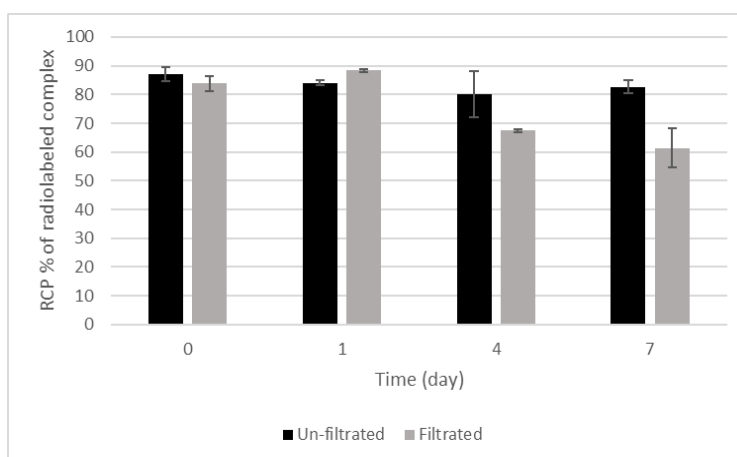


Figure 3. RCP % values of filtrated and un-filtrated radiolabeled complex (n=3).

Radiolabeling Stability

The separation of radionuclide from the pharmaceutical part is a critical problem since it causes the radionuclide can not to reach the targeted tissue. In addition to obtaining inadequate radioactive signals from targeted tissue, this separation gives rise to the uptake of unnecessary radioactivity in the healthy tissues due to free radionuclide localization. Therefore, the evaluation of radiolabeling should be performed (de Blois,

de Zanger, Chan, Konijnenberg, & Breeman, 2019). In our study, the RCP % value of ¹⁷⁷Lu-TDZ was calculated by the paper chromatography and HPLC 7 days after radiolabeling to evaluate the labeling stability of ¹⁷⁷Lu-TDZ in saline at room temperature. The RCP % values obtained from paper chromatography and HPLC are given in Table 3. Although over 80% RCP % value was calculated by paper chromatography at the beginning of the radiolabeling stability study, low-

er RCP % values were obtained from HPLC. In addition, according to the results of both HPLC and paper chromatography analyses, it was found that RCP % values significantly decreased on the 7th day ($p < 0.05$). In the literature, it was reported that the use of chelating agents such as DTPA and 1,4,7,10-tetraazacyclododecan-N,N',N'',N'''-tetraacetic acid (DOTA) increased the radiolabeling stability in the labeling process of ¹⁷⁷Lu (Kang et al., 2015; Watanabe, Hashimoto,

& Ishioka, 2015).

Furthermore, the HPLC chromatograms of free ¹⁷⁷Lu and ¹⁷⁷Lu-TDZ complex are given in Figure 4. Free ¹⁷⁷Lu chromatogram is presented in Figure 4A, and its retention time is 2.45 minutes. The second chromatogram showed a ¹⁷⁷Lu-CMS peak with 10.8 minutes retention time in addition to the peak of free ¹⁷⁷Lu displayed.

Table 3. RCP % values of filtrated ¹⁷⁷Lu-TDZ obtained from HPLC and paper chromatography.

Time (days)	HPLC	Paper chromatography
0	76.5 ± 6.9	83.9 ± 2.6
1	80.2 ± 7.7	67.4 ± 0.4
7	67.8 ± 5.7	61.5 ± 6.9

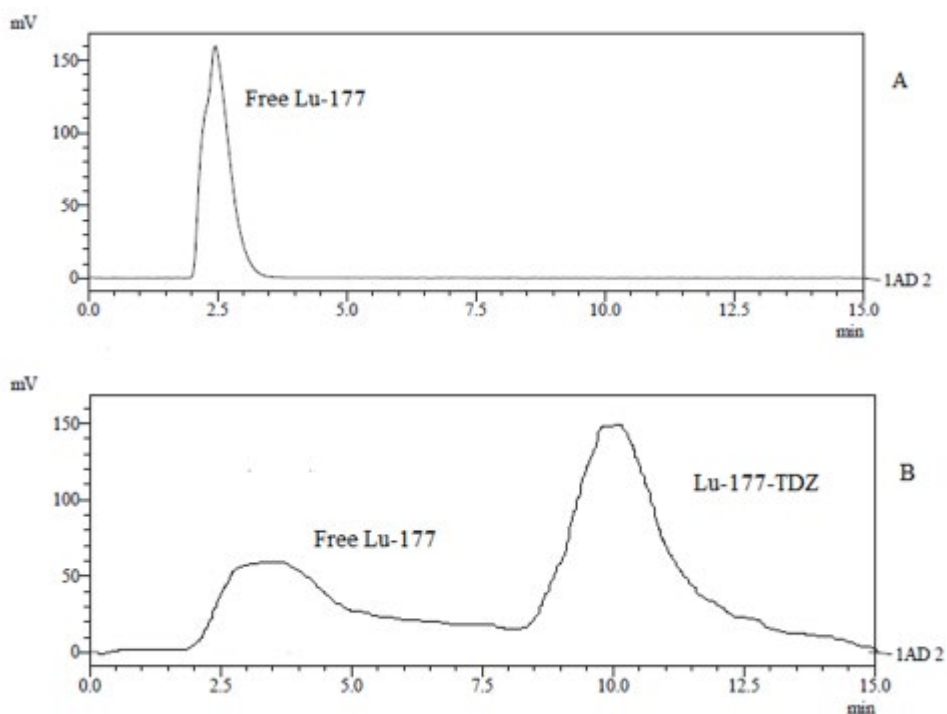


Figure 4. HPLC chromatograms of free ¹⁷⁷Lu (A) and ¹⁷⁷Lu-TDZ (B).

CONCLUSION

Globally, infection is still one of the significant health problems in view of Covid-19. The diagnosis and differentiation of infection from other pathologies is critically important to choose the appropriate treatment options, start the treatment in acute stages,

and follow the progression of the disease. Infection can be clinically diagnosed by biopsy, imaging techniques, biochemical tests, or symptomatic evaluation of patients. Imaging techniques present advantages such as their applicability to obtain whole-body images, ability to detect unknown infection focally, and

low risk compared to biopsy. In imaging systems, nuclear medicine techniques have been preferred due to providing functional and physiological images from tissues in addition to anatomical information. Therefore, the development of sensitive and specific radiopharmaceuticals is essential to image infection at molecular stages. Although infection treatment can be performed by the use of various antibiotic molecules, the severe side effects of antibiotics and the development of antimicrobial resistance limit treatment efficiency. Theranostic systems, consisting of therapeutic and diagnostic agents, have become crucial in recent years due to their advantages.

Hence, in our study, a theranostic radiopharmaceutical, containing TDZ and ^{177}Lu , was developed to image SPECT or gamma camera and treat the infection. In the experimental part, different incubation periods and chromatographic conditions were evaluated, and 60 min of incubation period was selected as the optimum time to obtain high RCP. In addition, ITLC-SG and ammonium hydroxide: methanol: water and DTPA solutions were chosen as the stationary and mobile phases, respectively, to detect amounts of impurities. Although over 80 % RCP was achieved in the radiolabeling efficiency study, the radiolabeling efficiency of the filtration complex significantly decreased over time. Therefore, the radiolabeled complex should be filtrated just before the administration to avoid this undesirable decrease in radiolabeling stability. Furthermore, in the HPLC chromatogram, two different peaks were observed depending on retention times of the free ^{177}Lu and ^{177}Lu -TDZ complex, but the radiolabeled complex did not exhibit stability for 7 days. Therefore, the addition of a chelating agent in radiolabeling conditions was suggested to increase the radiolabeling efficiency and stability. Thus, ^{177}Lu -TDZ can be a promising radiopharmaceutical in the treatment and imaging of difficult-to-reach and difficult-to-treat infections such as joint infections.

ACKNOWLEDGEMENT

The authors wish to thank Assoc. Prof. Dr. Zeynep Şenyiğit for the generous gift of TDZ.

CONFLICT OF INTEREST

All the authors of this article declared no conflict of interest.

AUTHOR CONTRIBUTION STATEMENT

Conception and design (Karpuz, M., Ozgenc, E., Atlihan-Gundogdu, E.), data collection and processing (Ozgenc, E., Atlihan-Gundogdu, E., Burak Z), analysis and interpretation (Karpuz, M., Ozgenc, E., Atlihan-Gundogdu, E), literature search (Karpuz, M.), preparing the study text (Karpuz, M.), critical reviews (Atlihan-Gundogdu, E., Burak, Z).

REFERENCES

- Aerts, J., Ballinger, J. R., Behe, M., Decristoforo, C., Elsinga, P. H., Faivre-Chauvet, A., . . . European Association of Nuclear, M. (2014). Guidance on current good radiopharmacy practice for the small-scale preparation of radiopharmaceuticals using automated modules: a European perspective. *J Labelled Comp Radiopharm*, 57(10), 615-620. doi:10.1002/jlcr.3227
- Akbar, M. U., Bokhari, T. H., Khalid, M., Ahmad, M. R., Roohi, S., Hina, S., . . . Jabbar, T. (2017). Radiolabeling, quality control, and biological characterization of (^{177}Lu) Lu-labeled kanamycin. *Chem Biol Drug Des*, 90(3), 425-431. doi:10.1111/cbdd.12960
- Banerjee, S., Pillai, M. R., & Knapp, F. F. (2015). Lutetium-177 therapeutic radiopharmaceuticals: linking chemistry, radiochemistry, and practical applications. *Chem Rev*, 115(8), 2934-2974. doi:10.1021/cr500171e
- Bart, S. M., Rubin, D., Kim, P., Farley, J. J., & Nambiar, S. (2020). Trends in Hospital-Acquired and Ventilator-Associated Bacterial Pneumonia Trials. *Clin Infect Dis*, 73(3), e602-e608. doi:10.1093/cid/ciaa1712

- Breeman, W. A., De Jong, M., Visser, T. J., Erion, J. L., & Krenning, E. P. (2003). Optimising conditions for radiolabelling of DOTA-peptides with ^{90}Y , ^{111}In and ^{177}Lu at high specific activities. *Eur J Nucl Med Mol Imaging*, 30(6), 917-920. doi:10.1007/s00259-003-1142-0
- Bryant, A. E., Bayer, C. R., Aldape, M. J., McIndoo, E., & Stevens, D. L. (2020). Emerging erythromycin and clindamycin resistance in group A streptococci: Efficacy of linezolid and tedizolid in experimental necrotizing infection. *J Glob Antimicrob Resist*, 22, 601-607. doi:10.1016/j.jgar.2020.04.032
- Cada, D. J., Ingram, K., & Baker, D. E. (2014). Tedizolid phosphate. *Hosp Pharm*, 49(10), 961-971. doi:10.1310/hpj4910-961
- de Blois, E., de Zanger, R. M. S., Chan, H. S., Konijnenberg, M., & Breeman, W. A. P. (2019). Radiochemical and analytical aspects of inter-institutional quality control measurements on radiopharmaceuticals. *EJNMMI Radiopharm Chem*, 4(1), 3. doi:10.1186/s41181-018-0052-1
- Gutfilen, B., Souza, S. A., & Valentini, G. (2018). Copper-64: a real theranostic agent. *Drug Des Devel Ther*, 12, 3235-3245. doi:10.2147/DDDT.S170879
- Hu, F., Cutler, C. S., Hoffman, T., Sieckman, G., Volkert, W. A., & Jurisson, S. S. (2002). Pm-149 DOTA bombesin analogs for potential radiotherapy: in vivo comparison with Sm-153 and Lu-177 labeled DO3A-amide- β Ala-BBN(7-14)NH₂. *Nucl Med Biol*, 29(4), 423-430. doi:10.1016/S0969-8051(02)00290-1
- Jones, R. N. (2010). Microbial Etiologies of Hospital-Acquired Bacterial Pneumonia and Ventilator-Associated Bacterial Pneumonia. *Clin Infect Dis*, 51(Supplement_1), S81-S87. doi:10.1086/653053
- Kang, C. S., Chen, Y., Lee, H., Liu, D., Sun, X., Kweon, J., . . . Chong, H. S. (2015). Synthesis and evaluation of a new bifunctional NETA chelate for molecular targeted radiotherapy using ^{90}Y or ^{177}Lu . *Nucl Med Biol*, 42(3), 242-249. doi:10.1016/j.nucmedbio.2014.10.004
- Karpuz M., Ozgenc E., Atlihan-Gundogdu, E., Burak Z. (2022). Pre-study on radiolabeling of colistin with Lutetium-177 to develop theranostic infection agent. *J Res Pharm*, 26(2), 397-407. doi:http://dx.doi.org/10.29228/jrp.137
- Karpuz, M., & Silindir-Gunay, M. (2022). Lipid-Based Drug Delivery Systems and Their Role in Infection and Inflammation Imaging. In *Nanoengineering of Biomaterials* (pp. 469-503).
- Kassis, A. I. (2008). Therapeutic radionuclides: biophysical and radiobiologic principles. *Semin Nucl Med*, 38(5), 358-366. doi:10.1053/j.semnuclmed.2008.05.002
- Klähn, M., Mathias, G., Kötting, C., Nonella, M., Schlitter, J., Gerwert, K., & Tavan, P. (2004). IR Spectra of Phosphate Ions in Aqueous Solution: Predictions of a DFT/MM Approach Compared with Observations. *The J Phys Chem*, 108(29), 6186-6194. doi:10.1021/jp048617g
- Levine, R., & Krenning, E. P. (2017). Clinical History of the Theranostic Radionuclide Approach to Neuroendocrine Tumors and Other Types of Cancer: Historical Review Based on an Interview of Eric P. Krenning by Rachel Levine. *J Nucl Med*, 58(Suppl 2), 3S-9S. doi:10.2967/jnumed.116.186502
- Liu, C., Bayer, A., Cosgrove, S. E., Daum, R. S., Fridkin, S. K., Gorwitz, R. J., . . . Infectious Diseases Society of, A. (2011). Clinical practice guidelines by the infectious diseases society of america for the treatment of methicillin-resistant *Staphylococcus aureus* infections in adults and children. *Clin Infect Dis*, 52(3), e18-55. doi:10.1093/cid/ciq146

- Michalska, K., Mizera, M., Lewandowska, K., & Cielecka-Piontek, J. (2016). Infrared, Raman and ultraviolet with circular dichroism analysis and theoretical calculations of tedizolid. *J Mol Struct*, 1115, 136-143. doi:10.1016/j.molstruc.2016.02.098
- Mota, F., Jadhav, R., Ruiz-Bedoya, C. A., Ordonez, A. A., Klunk, M. H., Freundlich, J. S., & Jain, S. K. (2020). Radiosynthesis and Biodistribution of (18) F-Linezolid in Mycobacterium tuberculosis-Infected Mice Using Positron Emission Tomography. *ACS Infect Dis*, 6(5), 916-921. doi:10.1021/acscinfedis.9b00473
- Mulcahy, M. E., & McLoughlin, R. M. (2016). Staphylococcus aureus and Influenza A Virus: Partners in Coinfection. *mBio*, 7(6). doi:10.1128/mBio.02068-16
- Naqvi, S. A. R., Rasheed, R., Ahmed, M. T., Zahoor, A. F., Khalid, M., & Mahmood, S. (2017). Radiosynthesis and preclinical studies of ¹⁷⁷Lu-labeled sulfadiazine: a possible theranostic agent for deep-seated bacterial infection. *J Radioanal Nucl Chem*, 314(2), 1023-1029. doi:10.1007/s10967-017-5477-6
- Paczkowska-Walendowska, M., Rosiak, N., Tykarska, E., Michalska, K., Plazinska, A., Plazinski, W., . . . Cielecka-Piontek, J. (2020). Tedizolid-Cyclodextrin System as Delayed-Release Drug Delivery with Antibacterial Activity. *Int J Mol Sci*, 22(1). doi:10.3390/ijms22010115
- Shahzad, M. A., Naqvi, S. A. R., Rasheed, R., Yameen, M., Anjum, F., Ahmed, M. T., . . . Gillani, S. J. H. (2017). Radiolabeling of benzylpenicillin with lutetium-177: Quality control and biodistribution study to develop theranostic infection imaging agent. *Pak J Pharm Sci*, 30(6(Supplementary)), 2349-2354.
- Singh, V., Upadhyay, P., Reddy, J., & Granger, J. (2021). SARS-CoV-2 respiratory co-infections: Incidence of viral and bacterial co-pathogens. *Int J Infect Dis*, 105, 617-620. doi:10.1016/j.ijid.2021.02.087
- Srivastava, S., Cirrincione, K. N., Deshpande, D., & Gumbo, T. (2020). Tedizolid, Faropenem, and Moxifloxacin Combination With Potential Activity Against Nonreplicating Mycobacterium tuberculosis. *Front Pharmacol*, 11, 616294. doi:10.3389/fphar.2020.616294
- Tong, S. Y., Davis, J. S., Eichenberger, E., Holland, T. L., & Fowler, V. G., Jr. (2015). Staphylococcus aureus infections: epidemiology, pathophysiology, clinical manifestations, and management. *Clin Microbiol Rev*, 28(3), 603-661. doi:10.1128/CMR.00134-14
- Velikyan, I. (2014). Chapter 17 - Radionuclides for Imaging and Therapy in Oncology. In X. Chen & S. Wong (Eds.), *Cancer Theranostics* (pp. 285-325). Oxford: Academic Press.
- Watanabe, S., Hashimoto, K., & Ishioka, N. S. (2015). Lutetium-177 complexation of DOTA and DTPA in the presence of competing metals. *J Radioanal Nucl Chem*, 303(2), 1519-1521. doi:10.1007/s10967-014-3590-3
- Wu, M., & Shu, J. (2018). Multimodal Molecular Imaging: Current Status and Future Directions. *Contrast Media Mol Imaging*, 2018, 1382183. doi:10.1155/2018/1382183
- Wunderink, R. G., Roquilly, A., Croce, M., Rodriguez Gonzalez, D., Fujimi, S., Butterton, J. R., . . . De Anda, C. (2021). A Phase 3, Randomized, Double-Blind Study Comparing Tedizolid Phosphate and Linezolid for Treatment of Ventilated Gram-Positive Hospital-Acquired or Ventilator-Associated Bacterial Pneumonia. *Clin Infect Dis*, 73(3), e710-e718. doi:10.1093/cid/ciab032
- Xu, Q., Zhang, S., Zhao, Y., Feng, Y., Liu, L., Cai, L., . . . Chen, Y. (2019). Radiolabeling, quality control, biodistribution, and imaging studies of (¹⁷⁷) Lu-ibandronate. *J Labelled Comp Radiopharm*, 62(1), 43-51. doi:10.1002/jlcr.3694

- Yang, Z., Tian, L., Liu, J., & Huang, G. (2018). Construction and evaluation in vitro and in vivo of tedizolid phosphate loaded cationic liposomes. *J Liposome Res*, 28(4), 322-330. doi:10.1080/08982104.2017.1380665
- Yousefnia, H., Jalilian, A. R., Zolghadri, S., Bahrami-Samani, A., Shirvani-Arani, S., & Ghannadi-Maragheh, M. (2010a). Preparation and quality control of (1)(7)(7)Lu-[tris(1,10-phenanthroline)lutetium(III)] complex for therapy. *Nucl Med Rev Cent East Eur*, 13(2), 49-54.
- Yousefnia, H., Jalilian, A. R., Zolghadri, S., Bahrami-Samani, A., Shirvani-Arani, S., & Ghannadi-Maragheh, M. (2010b). Preparation and quality control of lutetium-177 bleomycin as a possible therapeutic agent. *Nukleonika*, 55(3), 285-291.